Available online at www.sciencedirect.com
ScienceDirect
Journal of Power Sources 180 (2008) 468–475
JOURNAL OF POWER SOURCES
www.elsevier.com/locate/jpowsour

Frequency control in micro-grid power system combined with electrolyzer system and fuzzy PI controller

Xiangjun Li [a,*], Yu-Jin Song [b], Soo-Bin Han [b]

[a] State Key Laboratory of Automotive Safety and Energy, Tsinghua University, Beijing 100084, China
[b] Electric Energy and Lighting Center, Korea Institute of Energy Research, Daejeon, Republic of Korea

Received 21 January 2008; received in revised form 26 January 2008; accepted 28 January 2008
Available online 16 February 2008

Abstract

The widespread use of various kinds of distributed power sources would impact the quality of the power supply within a micro-grid power system, causing many control problems. This paper focuses on the stability of micro-grid operation and discusses the control techniques of combining a micro-turbine with the fuel cell and electrolyzer hybrid system to expand the micro-grid system's ability to solve power quality issues resulting from frequency fluctuations. The paper examines the feasibility of fuel cell and electrolyzer hybrid system control, especially dynamic control of an electrolyzer system, to secure a real power balance and enhance the operational capability of load frequency control. The proposed control and monitoring system can be considered to be a means of power quality control, both to improve the frequency fluctuations caused by random power fluctuations on the generation and load sides and to relax tie-line power flow fluctuations caused by frequency fluctuations in the interconnected micro-grid power system.

Keywords: Power quality control; Micro-grid; Electrolyzer system; Fuzzy PI controller; Renewable energy

1. Introduction

Although the idea of effective renewable energy use as a means of coping with environmental and resource problems, especially of reducing CO_2 emissions, is globally attractive, inappropriate application of distributed generation power supply systems can be a cause of insecure power supply. The micro-grid is one such system, consisting of distributed generators, loads, power storage devices and heat recovery equipment, among other components [1–3]. The main advantages of the micro-grid system are that (1) it can be operated independently from conventional utility grids, (2) it can make use of power and heat sources collectively, (3) it can be interconnected to the utility grids at one point.

In this paper, a micro-grid system (see Fig. 1) comprised of a control and monitoring system, a micro-turbine, a housing load, a load-controllable electrolyzer system to manufacture hydrogen, a hydrogen tank and renewable-energy-utilizing generators such as 100 kW wind power (WP), 25 kW photovoltaic (PV), 5 kW proton exchange membrane fuel cell (FC), and others, is considered. We assume that the power supply–demand balance control of the micro-grid system is performed by the control and monitoring system through a control area network (CAN) composed communication network. Moreover, the electricity of electrolyzer system is supplied mainly by the wind power and photovoltaic energy sources and the hydrogen produced by the electrolyzer system is stored in the hydrogen tank to be converted back to electricity in the proton exchange membrane fuel cells. The wind power is considered as primary source. However, considering the lack of power supply from renewable power sources, a micro-turbine is implemented to supply the base load containing the electrolyzer system and the housing load. A 100 kW micro-gas turbine is considered and it is assumed that the fuel for this turbine is supplied independently by a micro-gas turbine system.

Wind and photovoltaic generators have the disadvantage of an unstable power output. Therefore, in these kinds of hybrid small-scale power systems, a sudden real power imbalance or a large frequency fluctuation can easily occur, and reducing such fluctuations by the sole means of applying the dynamic control

* Corresponding author. Tel.: +86 10 6278 5706; fax: +86 10 6278 5708.
E-mail address: xjLi79@hotmail.com (X. Li).

0378-7753/$ – see front matter © 2008 Elsevier B.V. All rights reserved.
doi:10.1016/j.jpowsour.2008.01.092

Nomenclature

Base	base capacity of micro-grid system
CAN	control area network
CMD	command
$dP_{Housing}$	standard deviation for housing real power
dP_{WP}	standard deviation for wind power output
dP_{PV}	standard deviation for PV output
D	damping coefficient
E	error
EC	error change
ES	electrolyzer system
Δf	frequency fluctuation
f_0	system frequency
FC	fuel cell
FPI	self-organizing fuzzy PI
K_E	quantificational gain for error
K_{EC}	quantificational gain for EC
K_{ES}	gain for ES
K_{FC}	gain for FC
K_I	integral gain
K_{MT}	droop property of MT output
K_P	proportional gain
ΔK_I	change in K_I
ΔK_P	change in K_P
M	inertia constant
MT	micro-turbine
NB	negative big
NM	negative medium
NS	negative small
PB	positive big
PEM	proton exchange membrane
PM	positive medium
PS	positive small
PV	photovoltaic
P_{ES}	load power of ES
P_{FC}	FC power output
$P_{Housing}$	load power of housing
P_{MT}	MT power output
P_{tie}	tie-line power
$P_{tie-ref}$	Scheduled P_{tie}
P_{WP}	wind power output
P^G	generated real power
P^L	system load
P_{ES}^{ini}	initial ES load power
P_{FC}^{ini}	initial FC output
$P_{Housing}^{ini}$	initial housing load
P_{MT}^{ini}	initial MT output
P_{PV}^{ini}	initial PV output
P_{WP}^{ini}	initial WP output
ΔP	real power imbalance
ΔP_{ES}	change in ES load
ΔP_{FC}	change in FC output
ΔP_{MT}	change in MT output
ΔP_{-ref}	expected ΔP in micro-grid
ΔP_{tie}	difference between P_{tie} and $P_{tie-ref}$
T_{ES}	time constant of ES
T_{FC}	time constant of FC
WP	wind power
X_{tie}	tie-line reactance
ZO	zero

Greek symbol

θ	relative phase angle between utility grid and micro-grid

of a micro-turbine is sometimes ineffective. Moreover, when the type of power line designed to be interconnected to a utility grid is 380 V three-phase AC line, applying a DC or AC source to the AC grid would lead to harmonic distortion of voltages and currents [4]. Thus, the widespread use of various kinds of distributed power sources would impact the quality of the power supply within the micro-grid, causing many control problems. Here, we have ignored the harmonics resulting mainly from the operation of power electronic systems (e.g. converters) and studied the frequency fluctuations resulting mainly from real power imbalances.

The so-called hydrogen economy is a long-term project that can be defined as an effort to change the current energy system to one which attempts to combine the cleanliness of hydrogen as an energy carrier with the efficiency of fuel cells as devices to transform energy into electricity and heat. As an energy carrier, hydrogen must be obtained from other energy sources, in processes that, at least in the long-term, avoid or minimize CO_2 emissions [5]. Electrolyzer system fed by renewable energies (such as photovoltaic solar panels or windmills) or biomass reformers is the distributed resource of interest to generate hydrogen.

A HOGEN® electrolyzer system [6] is considered in this paper. The power consumption of this system can be controlled in the millisecond level by adjusting the pressure in the customer piping system. This pressure control can be realized by means of a control and monitoring system operated

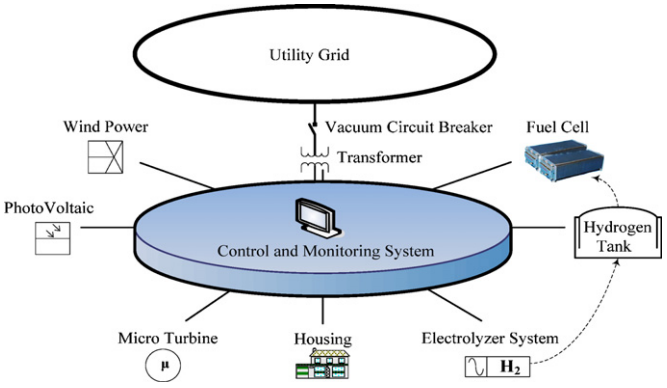

Fig. 1. System configuration of micro-grid network.

through a CAN composed communication network. Thereby, the electrolyzer system offers flexible controllability functions to compensate for system's real power imbalances. With regard to such a capability, this paper focuses on the stability of micro-grid operation, and proposes a combination of a micro-turbine and the fuel cell and electrolyzer hybrid system to deal with real-time frequency fluctuations and sudden real power imbalances.

PI and PID controllers are now used in approximately 90% of industrial control loops worldwide, because they offer good control system performance at an acceptable cost. The control system performance indices provided by the PI and PID controllers are not only the tuning parameters, but also the necessary implementation of additional functionalities including anti-windup, feedforward action, and set-point filtering [7]. Fuzzy control is a somewhat intelligent, cost-effective nonlinear control. Different types of adaptive fuzzy logic controls such as self-tuning and self-organizing controllers can be found in [8–15]. It is a known fact in PI-type controller configurations that when the integration factor is weak the system response will most probably be slow. However, when the integration factor is too strong the system response may fasten to a degree where system may become unstable [11]. Fuzzy control makes more sense to enhance conventional PID's performance by making up for the areas in which the PID gains do not do so well. The combination of a PI control and a fuzzy control strategy means that PI control has nonlinear characteristics and intellectual faculties, and simultaneously endows fuzzy control with an established PI-control configuration. The fuzzy self-tuning controller re-adjusts the PID gains in real-time to improve the process output response, during the system operation [12]. Therefore, it is considered that the fuzzy logic based self-tuning or self-organizing PI controller may overcome for the areas in which a PI controller alone is insufficient by providing an automatic adjusting method.

Here, self-organizing fuzzy PI (FPI) controllers, components in the control schemes of micro-turbine and tie-line power flow, are applied help to actualize the proposed control strategy more effectively. The effectiveness of the FPI controller will be investigated compared with the PI controller alone and open loop (no controller) through simulations.

This paper is organized as follows. Section 2 presents the formulation of power change by frequency fluctuation and that of random power fluctuation at generation and load sides. Section 3 presents the considered micro-grid power system model. Section 4 describes the FPI controllers. Simulation results are discussed in Section 5. Section 6 is the conclusions.

2. Problem formulation

Since frequency fluctuation, Δf, is effected mainly by the fluctuation of real power, power quality problems threatening frequency stability can be solved or avoided by satisfying the real power supply–demand balance constraint in the micro-grid power system. Therefore, an objective function for frequency control in the micro-grid system is formulized as follows:

$$\Delta P = P^{\mathrm{G}} - P^{\mathrm{L}} \to 0 \tag{1}$$

where

$$P^{\mathrm{G}} = P_{\mathrm{WP}} + P_{\mathrm{PV}} + P_{\mathrm{FC}} + P_{\mathrm{MT}} = P_{\mathrm{WP}} + P_{\mathrm{PV}} + P_{\mathrm{FC}}^{\mathrm{ini}} + P_{\mathrm{MT}}^{\mathrm{ini}} + (\Delta P_{\mathrm{FC}} + \Delta P_{\mathrm{MT}}) \tag{2}$$

$$P^{\mathrm{L}} = P_{\mathrm{Housing}} + P_{\mathrm{ES}} = P_{\mathrm{Housing}} + P_{\mathrm{ES}}^{\mathrm{ini}} + \Delta P_{\mathrm{ES}} \tag{3}$$

subject to

$$P_{\mathrm{WP}}^{\min} \le P_{\mathrm{WP}} \le P_{\mathrm{WP}}^{\max} \tag{4}$$

$$P_{\mathrm{PV}}^{\min} \le P_{\mathrm{PV}} \le P_{\mathrm{PV}}^{\max} \tag{5}$$

$$P_{\mathrm{FC}}^{\min} \le P_{\mathrm{FC}} \le P_{\mathrm{FC}}^{\max} \tag{6}$$

$$P_{\mathrm{MT}}^{\min} \le P_{\mathrm{MT}} \le P_{\mathrm{MT}}^{\max} \tag{7}$$

$$P_{\mathrm{ES}}^{\min} \le P_{\mathrm{ES}} \le P_{\mathrm{ES}}^{\max} \tag{8}$$

Because there are uncertainties in short-term load demand, in solar radiation and wind speed, although we have forecasted these profiles, there are deviations from the forecasted values in short-term operation. The deviations for wind power and housing loads are simulated close to an actual change wave by the following functions as presented in Ref. [16].

$$\mathrm{d}P_{\mathrm{WP}} = 0.8\sqrt{P_{\mathrm{WP}}} \tag{9}$$

$$\mathrm{d}P_{\mathrm{Housing}} = 0.6\sqrt{P_{\mathrm{Housing}}} \tag{10}$$

And the deviation from the forecasted PV power value is modeled similarly as follows:

$$\mathrm{d}P_{\mathrm{PV}} = 0.7\sqrt{P_{\mathrm{PV}}} \tag{11}$$

Therefore, in this paper, the input power variability of PV and WP is determined by considering the deviations from the forecasted values. And the following standard deviations, $\mathrm{d}P_{\mathrm{WP}}$, $\mathrm{d}P_{\mathrm{PV}}$, and $\mathrm{d}P_{\mathrm{Housing}}$ are multiplied by the random output fluctuation derived from the white noise block in MATLAB/SIMULINK in order to simulate the real-time random power fluctuation on the generation and load sides [16,17].

As shown in Eqs. (2) and (3), by controlling ΔP_{FC}, ΔP_{MT}, and ΔP_{ES} to meet the real-time power fluctuations on the generation (WP, PV) and load (housing) sides, Eq. (1) can be guaranteed. ΔP_{FC} and ΔP_{ES} are approximated by a first-order transfer function in reference to the operation of a battery-energy-storage facility, as shown in Ref. [18].

$$\Delta P_{\mathrm{FC}} = \frac{K_{\mathrm{FC}}}{1 + T_{\mathrm{FC}}s}\Delta f \tag{12}$$

$$\Delta P_{\mathrm{ES}} = \frac{K_{\mathrm{ES}}}{1 + T_{\mathrm{ES}}s}\Delta f \tag{13}$$

In this paper, the time constant of ES, T_{ES}, is a programmable setting parameter in the control and monitoring system and the value of T_{ES} is usually 60. However, as the above-mentioned, the power consumption of HOGEN® electrolyzer system can

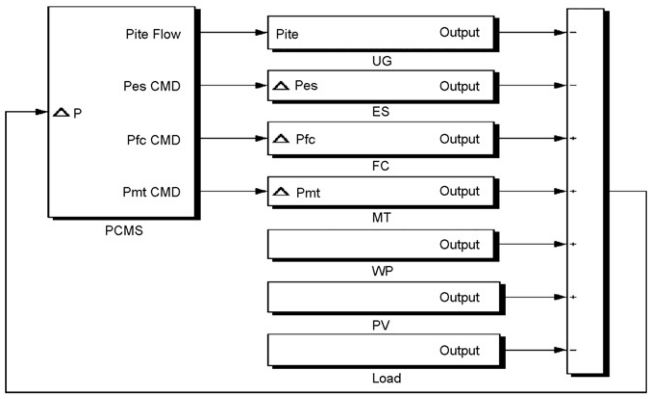

Fig. 2. Schematic diagram of micro-grid model system.

be controlled in the millisecond level. Therefore, to make full use of such high response controllability, the value of T_{ES} will be programmatically changed to 1 in such a case that there is a large frequency fluctuation in the micro-grid system.

In considering the linear P versus f droop characteristics, ΔP_{MT} is derived as follows:

$$\Delta P_{MT} = -\frac{1}{K_{MT}}\Delta f \tag{14}$$

Since the θ is obtained by

$$\theta = 2\pi f_0 \int \Delta f \, dt \tag{15}$$

the P_{tie} is derived from

$$P_{tie} = \frac{\sin(2\pi f_0 \, \Delta f/s)}{X_{tie}} \tag{16}$$

3. Specification of micro-grid system

A schematic diagram of the micro-grid system constructed by MATLAB/SIMULINK is shown in Fig. 2. The tie-line power and the dynamic behaviors of the electrolyzer system, fuel cell, and micro-turbine are assessed by the control and monitoring system according to the feedback parameter of ΔP.

A schematic diagram of the control and monitoring system is shown in Fig. 3. The parameters of the micro-grid model are shown in Table 1. The initial values of $P^{ini}_{Housing}$, P^{ini}_{WP}, and P^{ini}_{PV} are forecasted values as mentioned above. Moreover, in this paper, it is considered that the proton exchange membrane FC output power not use to the real-time control of ΔP and accordingly P_{FC} is set to a constant value of 5 kW in the course of a 500-s test.

4. Self-organizing fuzzy PI Controller

In this paper, two FPI controllers, Mamdani-type self-organizing controller, based on the fuzzy control principle and implemented with the fuzzy logic toolbox in MATLAB/SIMULINK, are introduced. A FPI controller related to ΔP compensation, for example, is shown in Fig. 4. The controller system consists of an adaptive PI controller and a fuzzy self-tuning mechanism and adjusts the parameters ΔK_P and ΔK_I on-line.

Tables 2 and 3 are the fuzzy rules for K_P and K_I, respectively. The fuzzy membership functions for FPI's input parameters (E and EC) and FPI's output parameters (ΔK_P and ΔK_I) are shown in Fig. 5. In FPI controller A, the initial values of K_P and K_I, to reduce ΔP, are 0.1 and 0.5, respectively, whereas, in FPI controller B, those initial values, to relax ΔP_{tie}, are 0.1 and 0.1, respectively. The initial values of K_P and K_I to be adjusted on-line by the FPI's output parameters ΔK_P and ΔK_I and therefore the PI controller action is updated after each cycle time. K_E and K_{EC} are 1000 and 100 respectively in Fig. 4. The ΔP and P_{tie} are measured at 5- and 4-s intervals, respectively, by setting the input signal delay time of the FPI controller, as shown in Fig. 4.

Table 1
Micro-grid model parameters

ES	
P^{ini}_{ES} (kW)	50
P^{max}_{ES} (kW)	70
P^{min}_{ES} (kW)	30
K_{ES}	100
T_{ES}	60
MT	
P^{ini}_{MT} (kW)	70
P^{max}_{MT} (kW)	100
P^{min}_{MT} (kW)	10
K_{MT}	0.04
M	10
D	1
Housing	
$P^{ini}_{Housing}$ (kW)	50
FC	
P^{ini}_{FC} (kW)	5
P^{max}_{FC} (kW)	5
P^{min}_{FC} (kW)	2
K_{FC}	–
T_{FC}	–
WP	
P^{ini}_{WP} (kW)	15
P^{max}_{WP} (kW)	100
PV	
P^{ini}_{PV} (kW)	10
P^{max}_{PV} (kW)	25
Tie-line	
X_{tie}	0.072
System	
f_0 (Hz)	50
Base	100

5. Simulation results

The initial real power balance in the micro-grid is set to zero at the simulation starting point, as shown in Table 1, and the feasibility of the electrolyzer system dynamic control is examined over the course of 500 s. The reference parameters $P_{tie-ref}$ and ΔP_{-ref} are set to zero. That is, in the case of interconnected operation with utility grid, the tie-line power flow target is zero.

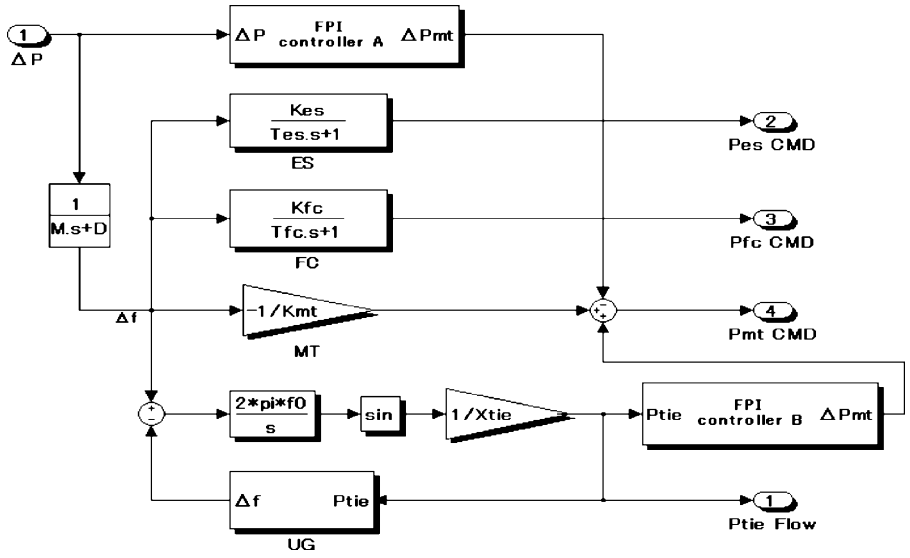

Fig. 3. Proposed control and monitoring system structure.

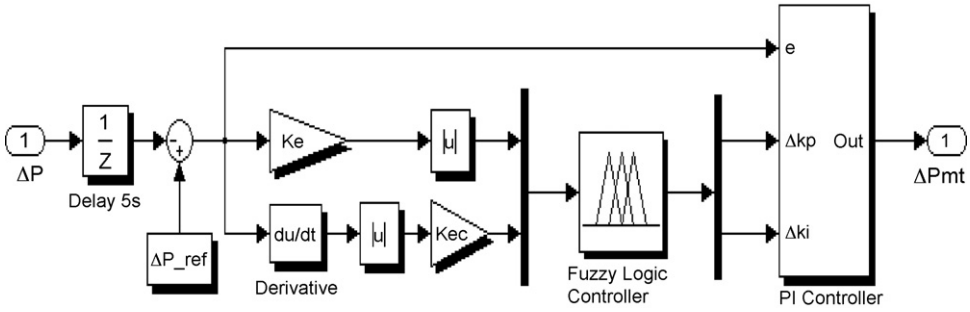

Fig. 4. FPI controller A related to ΔP compensation.

The simulation results for the two operational modes, islanding operation and utility-grid-connected operation, are presented as follows.

5.1. Case A: Islanding operation

Figs. 6 and 7 show the change of real power profile as a result of using electrolyzer system and FPI controls. Figs. 8 and 9 show the frequency fluctuations as a result of using electrolyzer system and FPI controls, respectively. For the well-tuned PI controller as shown in Fig. 9, the gain values of K_P and K_I, to reduce ΔP, are 0.1 and 0.5, respectively. Comparing Figs. 6 and 7 shows that the control and monitoring system controls the power consumption of the electrolyzer system to relax the load fluctuation, and changes the output power of the micro-turbine to match the real power balance. As shown in Figs. 8 and 9, the result is that the frequency fluctuation is reduced by the dynamic control of the electrolyzer system, and is additionally improved by applying the FPI controller A compared with the well-tuned PI controller alone and open loop (without PI controller).

Table 2
Fuzzy rule table (ΔK_P) for K_P

E	EC						
	NB	NM	NS	ZO	PS	PM	PB
NB	PB	PB	PB	PM	PS	ZO	ZO
NM	PB	PB	PM	PS	PS	ZO	NS
NS	PM	PM	PM	PS	ZO	NS	NS
ZO	PM	PM	PS	ZO	NS	NM	NM
PS	PS	PS	ZO	NS	NS	NM	NM
PM	PS	ZO	NS	NM	NM	NM	NB
PB	ZO	ZO	NM	NM	NM	NB	NB

Table 3
Fuzzy rule table (ΔK_I) for K_I

E	EC						
	NB	NM	NS	ZO	PS	PM	PB
NB	NB	NB	NM	NM	NS	ZO	ZO
NM	NB	NB	NM	NS	NS	ZO	ZO
NS	NB	NM	NS	NS	ZO	PS	PS
ZO	NM	NM	NS	ZO	PS	PM	PM
PS	ZO	ZO	ZO	NS	NS	ZO	ZO
PM	NS	NS	NS	NS	ZO	ZO	ZO
PB	ZO	ZO	ZO	ZO	ZO	ZO	ZO

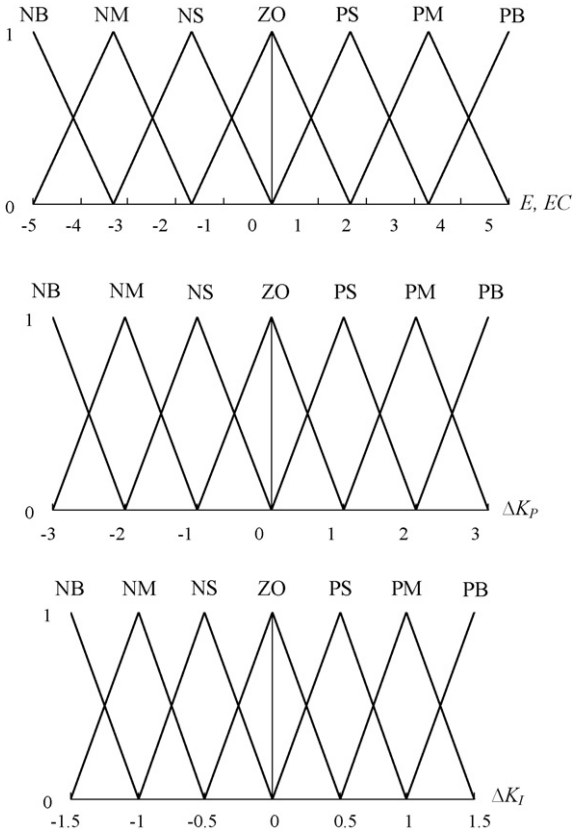

Fig. 5. Fuzzy membership function.

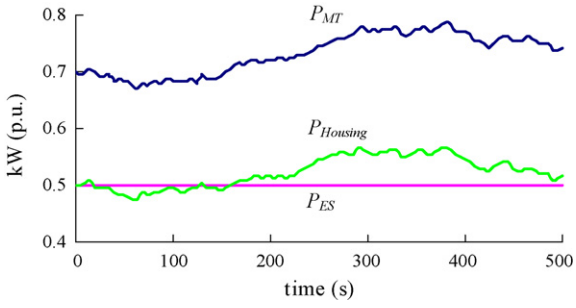

Fig. 6. Simulation result for islanding operation (case A): power profile without electrolyzer system and FPI control.

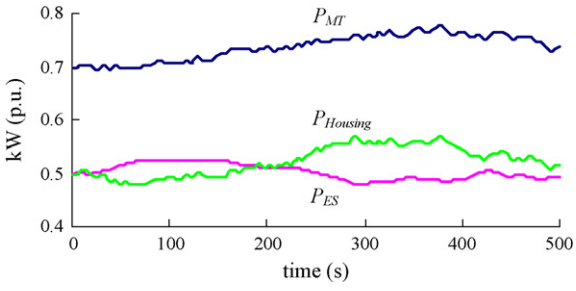

Fig. 7. Simulation result for islanding operation (case A): power profile with electrolyzer system and FPI control.

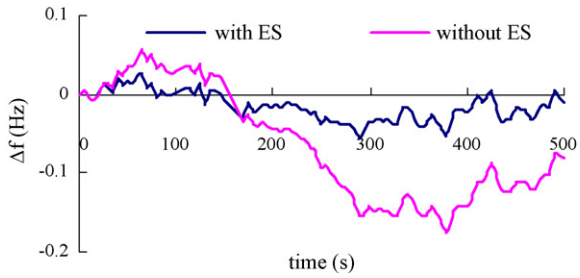

Fig. 8. Δf with or without electrolyzer system control for case A.

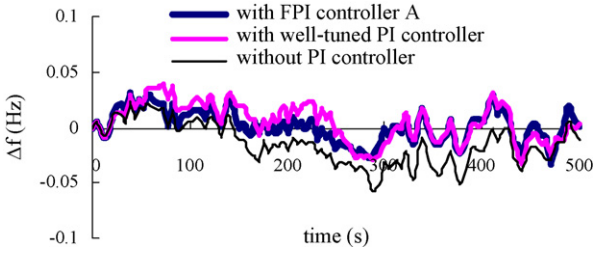

Fig. 9. Δf with or without FPI controller A for case A.

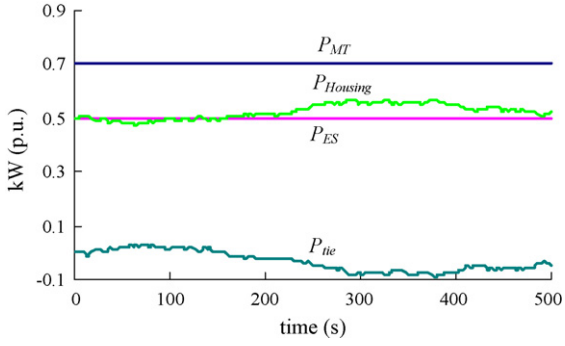

Fig. 10. Simulation results for utility grid connected operation (case B): power profile without FPI controller B.

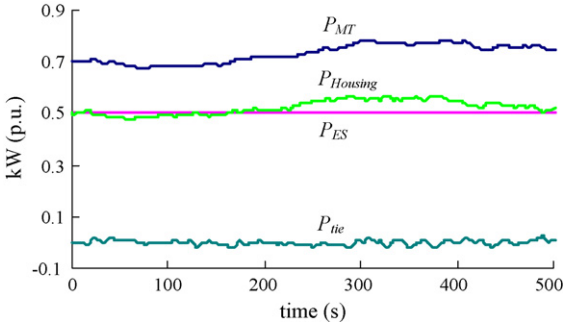

Fig. 11. Simulation results for utility grid connected operation (case B): power profile with FPI controller B.

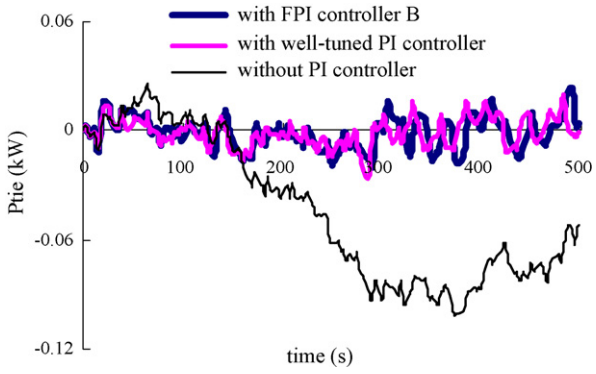

Fig. 12. Simulation results for utility grid connected operation (case B): tie-line power fluctuation with or without FPI controller B.

5.2. Case B: Utility grid connected operation

Figs. 10 and 11 show the change of real power profile as a result of applying FPI controller B. For convenience, the fuzzy membership function shown in Fig. 5 was also used in FPI controller B. Comparing Figs. 10 and 11 shows that, using FPI controller B to adjust the power output of the micro-turbine, the power supply from the utility grid is decreased. Fig. 12 is a magnified view of the P_{tie} fluctuation. In Fig. 12, for the well-tuned PI controller, the gain values of K_P and K_I, to relax ΔP_{tie}, are 0.1 and 0.1, respectively. It is obviously apparent that the tie-line power fluctuation is improved by introducing well-tuned PI controller and is little changed by introducing FPI controller B compared with the well-tuned PI controller alone. Fig. 13 shows the WP, PV, and FC outputs under the two above-mentioned operational modes.

5.3. Case C: Discussion for setting T_{ES}

For the above-mentioned two cases A and B, the T_{ES} was set to 60 to adjust the power consumption of the electrolyzer system according to a slow response time. A fast frequency fluctuation cannot be adequately repressed by means of generator governors and slow-response power sources. Since the load power of the electrolyzer system considered in this paper can be controlled at the millisecond level, the control and monitoring system can adjust the load power rapidly by changing the

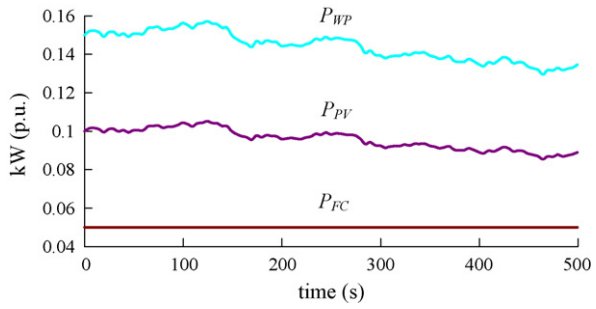

Fig. 13. WP, PV, and FC outputs in both operation models.

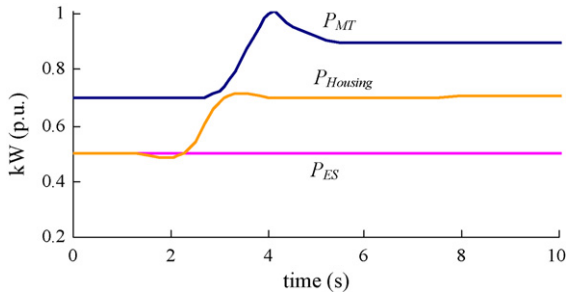

Fig. 14. Simulation results for setting TES (case C): power profile without electrolyzer system control.

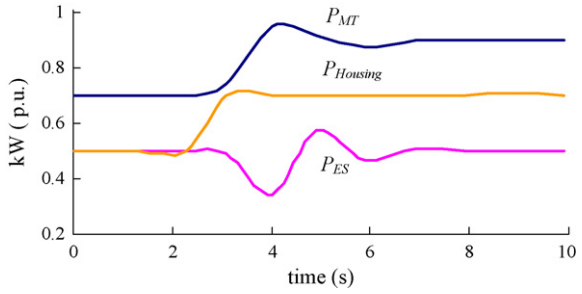

Fig. 15. Simulation results for setting TES (case C): power profile with electrolyzer system control.

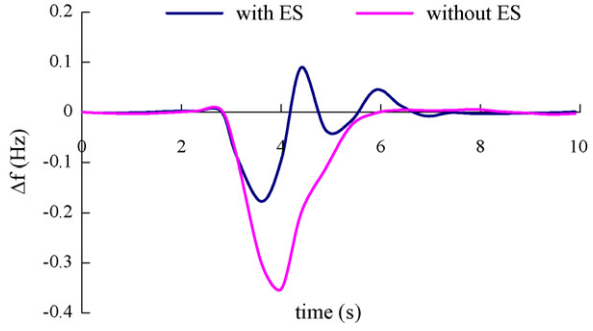

Fig. 16. Δf with or without electrolyzer system control for case C.

T_{ES} to a smaller value. Therefore, a case C, in which the T_{ES} is set to 1, is discussed below.

In this case, a sudden 20 kW overload at the third second, resulting in a fast and large frequency fluctuation in the micro-grid system, is simulated. Figs. 14–16 show the power profile and the frequency fluctuation before and after the electrolyzer system dynamic controls are considered, respectively. It appears that the maximum frequency fluctuation of 0.35 Hz is reduced effectively by utilizing the electrolyzer system's fast-response capability for kW load control.

6. Conclusions

In this paper, an electrolyzer system's dynamic control method, which secures a real power balance and enhances the operational capability to handle frequency fluctuation in multiple renewable energy hybrid micro-grid power system, is

proposed. The contents of this paper can be summarized as follows:

(1) The output changes of the fuel cell and the electrolyzer system are defined according to a first-order transfer function. The tie-line power and the output change of the micro-turbine according to the frequency fluctuation are presented.
(2) FPI controllers A and B are proposed to compensate the power changes in the micro-grid power system and tie-line. The effects of their use are also explored.
(3) The fluctuations of frequency and tie-line power under the islanding and interconnected operational modes, respectively, are considered in demonstrating the effectiveness of the proposed control scheme. It is concretely shown that a power quality improvement for frequency can be achieved by actively utilizing the load-controllable electrolyzer system. Therefore, the proposed control scheme helps to solve power quality issue resulting from frequency fluctuations.
(4) It is considered that in shorter periods in which sudden, large frequency fluctuations occur, applying a smaller T_{ES} to rapidly control the electrolyzer system load is a means of enhancing the operational capability to handle frequency fluctuations.

The efficient use of the fuel cell and electrolyzer hybrid system considering the state of charge for the hydrogen tank and the fluctuation of the voltage in the micro-grid system will be examined in the near future. Furthermore, the means by which the unit commitment of the multiple power sources can be determined to obtain an optimal daily operation schedule for a micro-grid power system will be discussed.

Acknowledgement

The authors would like to thank Mr. R. Melusky of Distributed Energy Systems Co. for his technical help of HOGEN® series devices.

References

[1] R.H. Lasseter, A. Akhil, C. Marnay, J. Stephens, J. Dagle, R. Guttromson, A.S. Meliopoilous, R. Yinger, J. Eto, Integration of Distributed Energy Resources–The CERTS MicroGrid Concept, April (2002) CERTS white paper.
[2] R.H. Lasseter, P. Paigi, Proceedings of the 35th Annual Conference IEEE PESC'04, 2004, pp. 4285–4290.
[3] X. Li, Y.-J. Song, S.-B. Han, IEEE PowerTech07, 2007 (ProCD No. 351).
[4] N.G. Hingorani, L. Gyugyi, Understanding FACTS-Concepts and Technology of Flexible AC Transmission Systems, IEEE Press, New York, 2000.
[5] G. Marban, T. Valdes-Solis, Int. J. Hydrogen Energy 32 (2007) 1625–1637.
[6] http://www.distributed-energy.com.
[7] R. Precup, S. Preitl, Inform. Sci. 177 (2007) 4410–4429.
[8] S.-J. Huang, H.-Y. Chen, Mechatronics 16 (2006) 607–622.
[9] S. Ziwei, C. Sizong, Y. Lin, Mach. Electric Eng. 35 (2006) 67–70 (in Chinese).
[10] Y. Yongmei, C. Ning, Comput. Inform. 21 (2005) 61–63 (in Chinese).
[11] M. Guzelkaya, I. Eksin, E. Yesil, Eng. Appl. Artif. Intell. 16 (2003) 227–236.
[12] H.B. Kazemian, ISA Trans. 40 (2001) 245–253.
[13] R.K. Mudia, N.R. Palb, Fuzzy Sets Syst. 121 (2001) 149–159.
[14] R.K. Mudia, N.R. Pal, Fuzzy Sets Syst. 115 (2000) 327–338.
[15] H.-Y. Chung, B.-C. Chen, J.-J. Lin, Fuzzy Sets Syst. 93 (1998) 23–28.
[16] T. Shinji, T. Sekine, A. Akisawa, T. Kashiwagi, G. Fujita, M. Matsubara, IEEJ Trans. PE 126 (1) (2006) (in Japanese).
[17] M. Matsubara, G. Fujita, T. Shinji, T. Sekine, A. Akisawa, T. Kashiwagi, R. Yokoyama, Proceedings of the 13th International Conference ISAP'05, 2005, pp. 67–72.
[18] D. Kottick, M. Blau, D. Edelstein, IEEE Trans. Energy Conv. 8 (September) (1993) 455–459.